

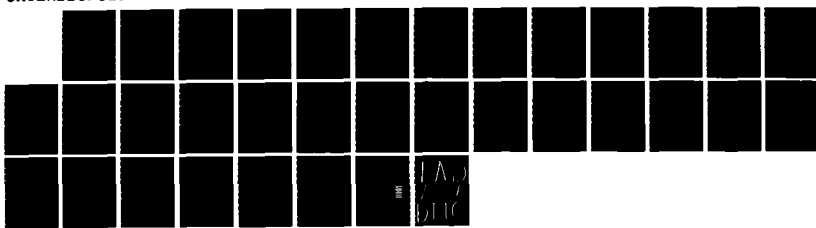
AD-A174 934

RADIATIVE PROCESSES FOLLOWING LASER EXCITATION OF THE A 1/1  
STATE OF PO(U) ARMY BALLISTIC RESEARCH LAB ABERDEEN  
PROVING GROUND MD K N HONG ET AL. OCT 86 BRL-TR-2766

UNCLASSIFIED

F/G 7/4

NL



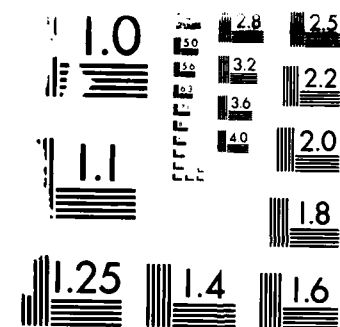
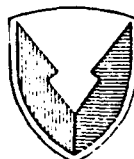


FIG. 1. Resolution Test Chart  
 (NBS 1963, p. 10)



US ARMY  
MATERIEL  
COMMAND

AD F 300853

9

TECHNICAL REPORT BRL-TR-2766

AD-A174 934

# RADIATIVE PROCESSES FOLLOWING LASER EXCITATION OF THE A STATE OF PO

Koon Ng Wong  
William R. Anderson  
Anthony J. Kotlar

October 1986

DTIC  
ELECTE  
DEC 11 1986  
S B

APPROVED FOR PUBLIC RELEASE; DISTRIBUTION UNLIMITED.

US ARMY BALLISTIC RESEARCH LABORATORY  
ABERDEEN PROVING GROUND, MARYLAND

86 12 11 04

DTIC FILE COPY

Destroy this report when it is no longer needed.  
Do not return it to the originator.

Additional copies of this report may be obtained  
from the National Technical Information Service,  
U. S. Department of Commerce, Springfield, Virginia  
22161.

The findings in this report are not to be construed as an official  
Department of the Army position, unless so designated by other  
authorized documents.

The use of trade names or manufacturers' names in this report  
does not constitute indorsement of any commercial product.

UNCLASSIFIED

SECURITY CLASSIFICATION OF THIS PAGE

ADA 174934

REPORT DOCUMENTATION PAGE				Form Approved OMB No 0704-0188 Exp Date Jun 30, 1986	
1a REPORT SECURITY CLASSIFICATION Unclassified			1b. RESTRICTIVE MARKINGS		
2a SECURITY CLASSIFICATION AUTHORITY			3 DISTRIBUTION / AVAILABILITY OF REPORT Approved for Public Release; Distribution Unlimited.		
2b DECLASSIFICATION / DOWNGRADING SCHEDULE					
4 PERFORMING ORGANIZATION REPORT NUMBER(S) Technical Report BRL-TR-2766			5. MONITORING ORGANIZATION REPORT NUMBER(S)		
6a NAME OF PERFORMING ORGANIZATION US Army Ballistic Research Laboratory		6b. OFFICE SYMBOL (If applicable) SLCBB-IB		7a. NAME OF MONITORING ORGANIZATION	
6c. ADDRESS (City, State, and ZIP Code)  Aberdeen Proving Ground, MD 21005-5066		7b. ADDRESS (City, State, and ZIP Code)			
8a. NAME OF FUNDING / SPONSORING ORGANIZATION		8b. OFFICE SYMBOL (If applicable)		9. PROCUREMENT INSTRUMENT IDENTIFICATION NUMBER	
8c. ADDRESS (City, State, and ZIP Code)		10. SOURCE OF FUNDING NUMBERS			
		PROGRAM ELEMENT NO. 61102A		PROJECT NO. A71A	
		TASK NO.		WORK UNIT ACCESSION NO.	
11 TITLE (Include Security Classification) RADIATIVE PROCESSES FOLLOWING LASER EXCITATION OF THE A STATE OF PO					
12 PERSONAL AUTHOR(S) Koon Ng. Wong*, William R. Anderson, Anthony J. Kotlar					
13a TYPE OF REPORT Final		13b TIME COVERED FROM Jan 83 TO Dec 85		14 DATE OF REPORT (Year, Month, Day) October 1986	
15. PAGE COUNT 29					
16 SUPPLEMENTARY NOTATION *NRC Postdoctoral Research Associate Published in Journal of Chemical Physics					
17 COSATI CODES			18. SUBJECT TERMS (Continue on reverse if necessary and identify by block number)		
FIELD	GROUP	SUB-GROUP			
07	04		PO Radical, Laser Induced Fluorescence, Radiative Lifetimes, Relative Emission Intensities		
19 ABSTRACT (Continue on reverse if necessary and identify by block number)					
<p>Laser induced fluorescence in the (0,0) band of the A doublet sigma plus - X doublet pi system of the PO radical (~2470 Angstroms) has been used to study the radiative properties of the A state. Detection of fluorescence from the PO radical is of military interest because of the central role it plays in several proposed laser photolysis detection schemes for nerve agents. In this paper, results of measurements of several key parameters necessary for quantitative detection of PO via laser induced fluorescence in the A-X system are presented. A laser excitation scan of the (0,0) band and a fluorescence scan of the emission are given. Fluorescence from the B doublet sigma plus state to the X state was observed (~3250 Angstroms) when the A state was pumped by the laser. The branching ratio for emission from the A state to the lower B and X states was indirectly determined. The A state was found to have a very short free radiative lifetime, <math>9.68 \pm 0.47</math> ns. In the absence of quenching, the excited state decay is found to be primarily due to radiative processes. Upper limits were determined for the quenching rates of Ar and He carrier.</p>					
20 DISTRIBUTION / AVAILABILITY OF ABSTRACT <input type="checkbox"/> UNCLASSIFIED/UNLIMITED <input checked="" type="checkbox"/> SAME AS RPT <input type="checkbox"/> DTIC USERS			21 ABSTRACT SECURITY CLASSIFICATION Unclassified		
22a NAME OF RESPONSIBLE INDIVIDUAL DR. WILLIAM R. ANDERSON			22b TELEPHONE (include Area Code) 301-278-6642		22c OFFICE SYMBOL SLCBB-IB-1

DD FORM 1473, 84 MAR

83 APR edition may be used until exhausted  
All other editions are obsoleteSECURITY CLASSIFICATION OF THIS PAGE  
UNCLASSIFIED

19. Abstract:

gases. Relative intensities of emission of the  $v'=0$  progression in the A-X system were also measured. These intensities were used to determine the electronic transition moment function in the region of the equilibrium internuclear distance.

# TABLE OF CONTENTS

	<u>Page</u>
LIST OF FIGURES.....	5
I. INTRODUCTION.....	7
II. EXPERIMENTAL.....	8
III. RESULTS AND DISCUSSION.....	9
A. Identification of the $A^2\Sigma^+-X^2\Pi$ (0,0) Band Fluorescence.....	9
B. Lifetime Measurements for $A^2\Sigma^+$ PO.....	11
C. $A^2\Sigma^+-X^2\Pi$ Electronic Transition Moment Function.....	14
D. Relative Intensities of Emission from the $A^2\Sigma^+$ State to the $B^2\Sigma^+$ and $X^2\Pi$ States.....	17
IV. CONCLUSIONS.....	19
ACKNOWLEDGEMENTS.....	20
REFERENCES.....	21
DISTRIBUTION LIST.....	25



**DTIC**  
**ELECTE**  
**DEC 11 1986**  
**B**

Accession For	
NTIS	✓
DTIC	
Unannounced	
Justification	
By	
Distribution	
Availability	
Dist	
<b>A-1</b>	

# LIST OF FIGURES

<u>Figure</u>		<u>Page</u>
1	Potential Energy Diagram for the PO Radical.....	7
2	Laser Excitation Scan of the (0,0) Band in the A-X System of PO. (a) $A^2\Sigma^+-X^2\Pi_{1/2}$ Subband. (b) $A^2\Sigma^+-X^2\Pi_{3/2}$ Subband.....	10
3	Fluorescence Scan of the PO Electronic Systems.....	11
4	Fluorescence Decay Pulse from $v'=0$ of the $A^2\Sigma^+$ State.....	13
5	Plot of $(p_{v',v''}/q_{v',v''})^{1/2}$ vs. $\bar{r}$ for the $v'=0$ Progression in the A-X System of PO.....	16



## I. INTRODUCTION

Spectroscopy of the PO radical has been studied using laser induced fluorescence (LIF) in our laboratory for several years. This radical is of military importance because of its central role in several proposed laser photolysis detection schemes for nerve agents under atmospheric conditions.<sup>1</sup> A potential energy diagram for the radical is shown in Figure 1. Reports on our studies of the transition between the two lowest doublet states,  $B^2\Sigma^+-X^2\Pi$  ( $\sim 3250\text{\AA}$ ), have appeared previously.<sup>3,4</sup> In the present work, we report on studies of laser excitation of the  $A^2\Sigma^+$  state via the A-X transition at about  $2470\text{\AA}$ . This transition is of particular interest because in one of the proposed agent detection schemes,<sup>5</sup> a KrF excimer laser ( $\sim 2480\text{\AA}$ ) would be used both to photolyze the agent molecule and then to excite fluorescence of the PO thus formed.

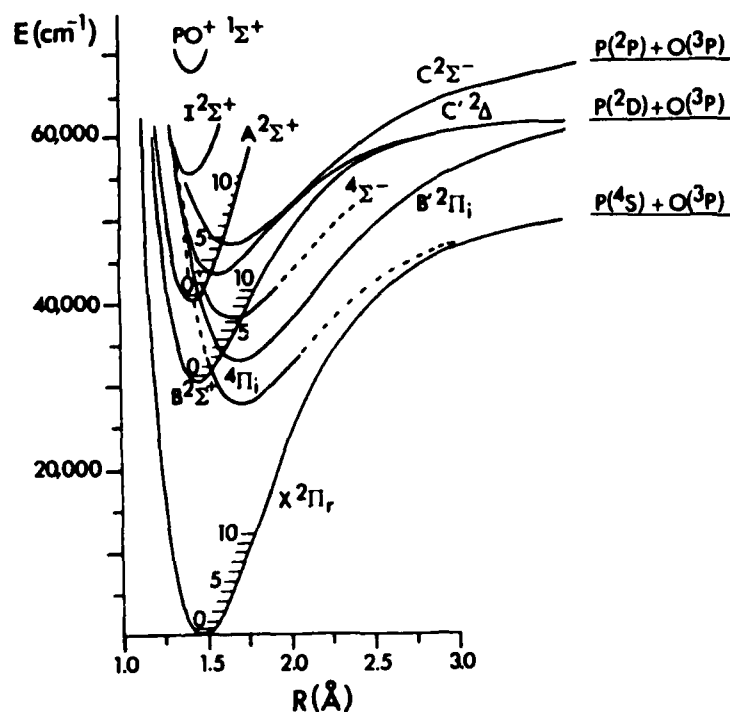


Figure 1. Potential Energy Diagram for the PO Radical.  
(Reproduced, with permission, from Ref. 2.)

Emission and absorption of the  $A^2\Sigma^+-X^2\Pi$  transition of PO has been studied at high resolution by Rao,<sup>6</sup> by Coquart and coworkers<sup>7</sup> and by Ghosh and Verma.<sup>8</sup> From these works, one may obtain much information about the vibrational and rotational constants for the states involved and about perturbations of the A state. Utility of the A-X transition as an analytical tool was studied by Winefordner and coworkers.<sup>9</sup> They used several flames as sources of PO. Most of the flames required the addition of P as phosphoric acid to produce PO, but acetylene generally contains a small fraction of  $\text{PH}_3$  impurity. Flames of acetylene were used for many of the studies, obviating

the need for addition of phosphoric acid. Fluorescence of PO was excited in the A-X system using a broadband xenon arc lamp. The fluorescence was dispersed by a medium resolution monochromator for study. The A-X fluorescence has since been studied under much higher resolution using laser sources. Recently, we reported on LIF studies of the A-X system.<sup>10</sup> Excitation and fluorescence scans and observation of B-X emission upon pumping the A state were reported. In addition, the first measurement of the A state radiative lifetime yielded "about 11.5 ns." (This measurement was good to 2.0 ns.) Shortly after this work, Long and coworkers<sup>11</sup> observed A-X system LIF of PO after excimer laser photolysis of dimethyl-methylphosphonate [DMMP;  $(\text{CH}_3\text{O})_2(\text{P}=\text{O})\text{CH}_3$ ]. Further excitation and fluorescence scans were given. The lifetime of the  $\text{A}^2\Sigma^+$  state was reported<sup>11a,b</sup> as  $9 \pm 2$  ns, in good agreement with our previous work. The transition between the  $\text{A}^2\Sigma^+$  and  $\text{B}^2\Sigma^+$  states is also allowed. High resolution emission studies of this transition have been performed by Verma and Jois.<sup>12</sup> The (0,0) band occurs at about 10,300Å. In addition to these experimental studies, there have also been several theoretical studies concerning the electronic structure of PO. Most of these include calculations on the A and B states. These papers were briefly reviewed in Ref. 4.

This paper concerns a much more detailed description of our work on the PO A-X system LIF than has appeared previously. Since our earlier work was reported, we have performed rotationally resolved measurements of the A state lifetime, relative intensity measurements for the  $v'=0$  progression of the A-X system, and we have measured the branching ratio for emission from the A state to the lower B and X states by an indirect method. Both previous measurements<sup>10,11a,b</sup> of the radiative lifetime may have been affected by waveform digitizer distortions of the type discussed in Ref. 4 since Tektronix waveform digitizers were used by both groups. The digitizer distortion was corrected in the present work. All of these studies of the A state LIF will be reported herein.

## II. EXPERIMENTAL

The experimental apparatus has been described in detail previously.<sup>4</sup> Only a brief description will be given here. For these experiments, PO was formed by flowing less than 1 micron of DMMP in inert carrier gas through a microwave discharge (2450 MHz). The resulting mixture then passed through a fluorescence cell. For most of the experiments Ar was used as the carrier, but occasionally He was used. The carrier pressure was about 2 torr except where otherwise noted. A Nd:YAG pumped dye laser system was used as the excitation source. The output of Rhodamine 640 laser dye was doubled to obtain radiation at  $\sim 3095\text{Å}$ . This radiation was then passed collinearly with the fundamental (6190Å) through a Raman shifter cell filled with  $\text{H}_2$ . The desired 2470Å radiation was obtained as the second anti-Stokes output from the cell. Under good conditions about 200  $\mu\text{J/pulse}$  of the desired radiation was obtained. The bandwidth was about  $0.3\text{ cm}^{-1}$ . This radiation was passed through the fluorescence cell where it excited PO in the A-X (0,0) band. Fluorescence was collected at 90 degrees from the excitation beam. For most of the experiments the fluorescence was focussed into a 32 cm monochromator equipped with a photomultiplier detector (PMT). For the A-X system excitation scan, the fluorescence was imaged directly through a bandpass filter, which transmitted only emission from the A-X system, into the PMT. This filter had

the following parameters: central wavelength  $\sim 2400\text{\AA}$ , FWHM  $\sim 380\text{\AA}$  and peak transmission  $\sim 22\%$ . Output of the PMT was processed by a boxcar averager for fluorescence or excitation scans or by a Tektronix 7912AD waveform digitizer for lifetime measurements. Boxcar averager and waveform digitizer outputs were stored on a laboratory computer for later analysis. The overall detector system response time for lifetime measurements was  $\sim 1.5$  ns. The fluorescence decay curves were corrected for digitizer distortion as discussed in Ref 4.

For the lifetime measurements, the detection system was carefully checked for any possible effects of saturation, such as space-charge effects in the phototube. This was done by scattering some of the laser radiation into the system. The intensity at the PMT was adjusted until the amplitude of the laser signal matched that of the fluorescence which was observed. No significant lengthening of the laser pulse, in comparison to low intensity pulses and to the output of a fast photodiode, was observed at the highest intensities used. Care was also taken to insure that the measurement of fluorescence branching ratios was not affected by self-absorption, which would cause fluorescence to the lowest vibrational levels to appear to be weaker than it actually is.

A significant amount of apparatus drift was noted during the first monochromator scans made to determine the relative intensities of emission from the  $v'=0$  level of the A state. In later scans a separate PMT was used in conjunction with the aforementioned filter to monitor the overall A-X system emission and thus monitor the experimental apparatus for drift. Output from the A-X monitor PMT was always processed by the boxcar averager. Both PMTs were carefully checked for possible saturation during relative intensity measurements. The detection system wavelength sensitivity was calibrated using an NBS traceable tungsten standards lamp for use in the relative intensity determinations.

### III. RESULTS AND DISCUSSION

#### A. Identification of the $A^2\Sigma^+-X^2\Pi$ (0,0) Band Fluorescence

The A-X (0,0) band fluorescence of PO was identified in both excitation and fluorescence scans. A laser excitation scan taken using the filtered PMT is given in Figure 2. Positive identification of the A-X system LIF is achieved by comparison of the observed spectrum in Figure 2 to line positions from earlier high resolution emission studies.<sup>6,7a</sup> Spin-splitting in both the  $B^2\Sigma^+$  and  $A^2\Sigma^+$  states is quite small. Ordinarily, 12 separate rotational branches are observed for a  $^2\Sigma-^2\Pi$  transition. However, four of these are satellite branches. Since the excited state spin-splitting is so small, the satellite branches are completely overlapped by the corresponding main branch transitions, even under high resolution.<sup>6,7a</sup> Only the main branch designations are given in Figure 2. The overlapped main plus satellite branch pairs are  $R_1+R_{021}$ ,  $Q_1+Q_{021}$ ,  $Q_2+Q_{R12}$  and  $P_2+P_{Q12}$ , respectively. The line positions in Figure 2 were taken from the vacuum wavenumbers in Ref. 7a. It should be noted that in one of the emission studies<sup>6</sup> and also the fluorescence excitation scan of Long and coworkers<sup>11b</sup> an incorrect conversion from vacuum wavenumbers to air wavelengths was performed. Figures of A-X vibrational band spectra in these papers are therefore incorrect by approximately 1Å. The correct air wavelengths are used in the present work. In addition, the

resolution in the present excitation scan is somewhat higher than that in Ref. 11b.

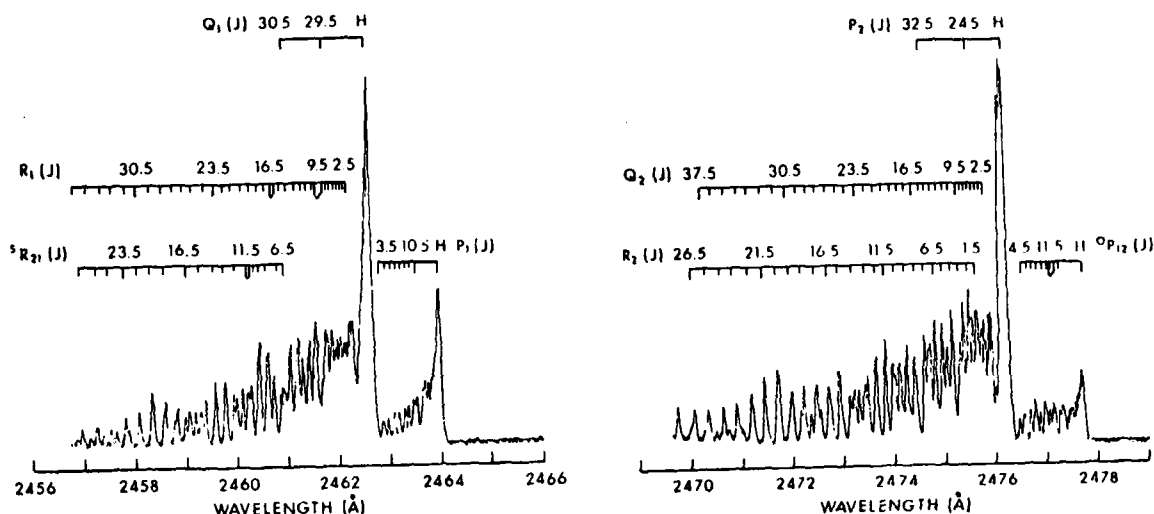


Figure 2. Laser Excitation Scan of the (0,0) Band in the A-X System of PO. (a)  $A^2\Sigma^+-X^2\pi_{1/2}$  Subband. (b)  $A^2\Sigma^+-X^2\pi_{3/2}$  Subband. There was no signal at room temperature between the two subbands. The scales for the two subbands are different. The  $^2\pi_{1/2}$  subband is actually somewhat stronger than the  $^2\pi_{3/2}$  subband, which may be attributed to the Boltzmann distribution in ground state spin-orbit levels.

A fluorescence scan of the  $v'=0$  emission in the A-X system is shown in Figure 3a. The scan was taken with the laser fixed to excite PO in the  $Q_1+P_{21}$  head of the (0,0) band, which is the strongest feature in the band (see Figure 2a). The monochromator was scanned using a resolution of about 6-7 Å FWHM. Band assignments were obtained from Ref. 13. Note that emission was readily observed to  $v''$  as high as 3 (see Figure 3a). Although careful intensity measurements were not performed on the (0,4) band (due to oversight), emission to  $v''=4$  could also be observed. This emission was much weaker than that of the bands shown in Figure 3a. In Figure 3a, one immediately notes a large splitting of the vibrational bands into doublets. This splitting arises from the  $\sim 224 \text{ cm}^{-1}$  spin-orbit splitting of the ground  $^2\pi$  state.<sup>6,7a</sup> The splitting is even more evident in the higher resolution excitation scans of Figure 2. There, one sees that the spin-orbit splitting is so large that the band is fully split into two distinct subbands at room temperature. In addition to the strong emission from the  $A^2\Sigma^+$  state, we found weaker emission from the  $B^2\Sigma^+$  state. A fluorescence scan of the B-X emission thus observed is shown in Figure 3b. This scan was taken at the same time and under the same conditions as that of Figure 3a. Of course, the B-X vibrational bands have a spin-orbit splitting similar to that of the A-X bands. This B-X splitting has been previously observed in emission<sup>14-16</sup> and LIF<sup>3,17</sup> studies. Questions immediately arise as to how the B state is

populated while the laser is pumping to the A state and what fraction of the molecules pumped to the A state find their way into the B state. Since radiative emission from the A state to the B state is allowed, as previously discussed, population of the B state may occur via radiative or collisional processes. Further discussion of these questions will be deferred to Section D.

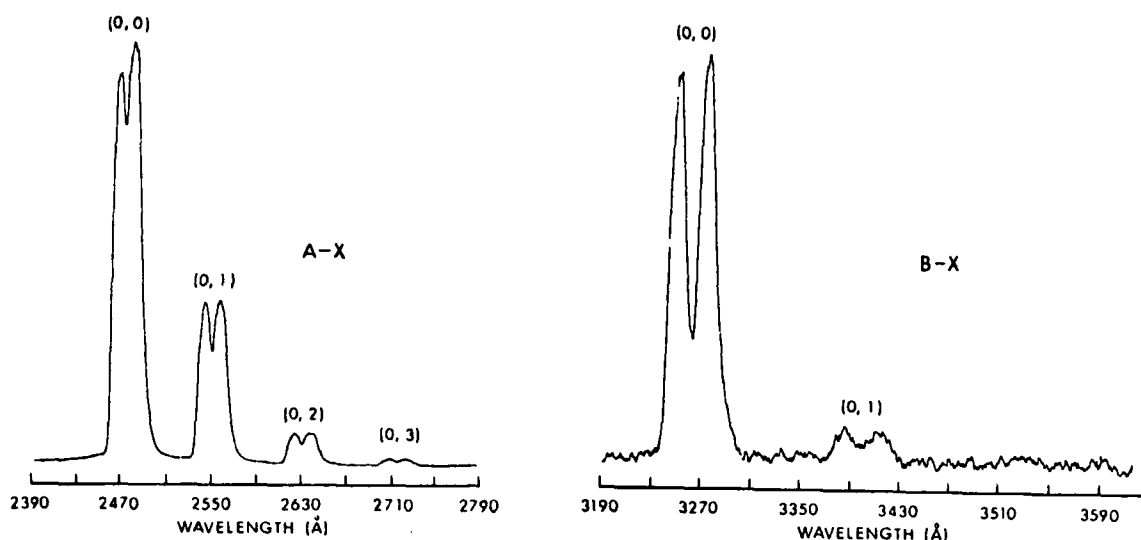


Figure 3. Fluorescence Scan of the PO Electronic Systems. The laser pumped the  $Q_1+Q_{21}$  head of the A-X (0,0) band and produced signal in both of the systems depicted. (a) A-X system fluorescence spectrum. (b) B-X system fluorescence spectrum. The B-X fluorescence was much weaker than that of the A-X system, resulting in a lower signal to noise ratio for the former.

#### B. Lifetime Measurements for $A^2\Sigma^+$ PO

$A^2\Sigma^+$  lifetime measurements were performed using the monochromator with wavelength set to observe the A-X (0,0) band fluorescence and slits set so that most of the band was being observed. Signals from the PMT were processed by the waveform digitizer and then averaged in the laboratory computer. Typically the signal to noise ratio was rather high so that only 100 pulses had to be averaged. In previous measurements<sup>4</sup> on the B state it was found that Tektronix 7912AD waveform digitizers introduce a small amount of distortion into the waveform due to an inherent nonlinearity. Though most intensity measurements are not affected by this small distortion, fits of exponential decays to obtain lifetimes are extremely sensitive to it. Systematic errors of 10-20% were frequently observed in the lifetimes when the

distorted waveforms were not corrected. Therefore, in the present work on the A state, the resultant waveforms were corrected for this distortion,<sup>4</sup> after the pulses were averaged, to obtain the true input waveform. We should note that such a correction was not used for either of the two previously reported measurements of the A state lifetime, in both of which 7912AD waveform digitizers were used.<sup>10,11a,b</sup> Therefore, systematic errors induced by digitizer distortion could have affected the results, although the exact magnitude of such errors is unknown. Fortunately, it will be seen shortly that all of the results are in reasonable agreement. Use of the deconvolution allows us to determine the lifetime with much higher precision than has been done previously. The system was always adjusted so that signals resulting from the weakest laser-driven transitions were optimized such that the signal level was high, yet the detection electronics were not quite saturated. The focussing lenses were then apertured when the laser was pumping the stronger transitions so that the resultant signals came to about this optimum level.

The first lifetime measurements were performed with the laser pumping in the  $Q_1 + Q_{P21}$  head. An example of the averaged output from the digitizer, after correction for distortion, is shown in Figure 4. A very fast fluorescence response followed by a slower decay to the baseline, typical of pulsed radiative lifetime measurements, was observed. A separate photodiode measurement of the laser excitation pulse shape was made in order to determine its width. The time it takes the photodiode response to rise above and fall below 1% of its maximum value was noted. In order to estimate the time at which fitting of the fluorescence signal by an exponential form would be permissible, we noted the point at which the signal began to rise rapidly, added the laser pulse duration as just defined and added a few ns more to insure insignificant response to laser excitation. (The same type of test was performed by scattering laser radiation into the monochromator with nearly identical results, but much lower signal to noise ratio since averaging was not performed. The main purpose of this latter test was to insure that detection system saturation did not give rise to the observed decays.) The tail of the decay pulse was fitted beginning at this point. The fit was performed in much the same manner as was done previously for the B state<sup>4</sup> using a nonlinear least squares routine<sup>18</sup> and the functional form

$$I = A \exp(-t/\tau) + B \quad (1)$$

where A is the signal amplitude, t is the elapsed time after the earliest point in the fit,  $\tau$  is the observed lifetime and B is the baseline. As may be seen in Figure 4, the lifetimes are of the order of 10 nsec. Since the detection system fall time was  $\sim 1.5$  nsec, as previously noted, concern arose that this response time might affect the measured lifetimes. However, calculations of Demas<sup>19</sup> show that the correct lifetime will be extracted if one delays fitting of the decay long enough after the excitation pulse. For these experiments, we were careful to insure that enough time had elapsed.

In order to be able to use the present lifetime measurements for the determination of absorption and emission coefficients, one must insure that all of the decay is due to radiative processes. We shall consider possible nonradiative channels here. Measurements of the decay constant vs. Ar carrier gas pressure (vide infra) show that the lifetime does not vary within its stated error limits in the range from 0.5-10 torr of carrier gas. Therefore, excited state quenching is unimportant. There is no possibility of

predissociation of  $v'=0$  in the A state because it is well below the limit for dissociation to ground state atoms (see Figure 1). Rotational perturbations are known<sup>7,12</sup> to occur in  $v'=0$  at  $N' = 10, 17$ , and  $55$ . The perturbations at  $N'=10$  and  $17$  are due to interaction between  $A^2\Sigma^+$  and  $b^4\Sigma^-$  while that at  $N'=55$  is not well understood. Since there are known perturbations it seemed possible that fast relaxation through the perturbed levels, i.e., as is known to occur between the  $B^2\Sigma^+$  and  $A^2\Sigma^+$  states of CN,<sup>20</sup> might affect the lifetimes. If this is the case, the lifetime of the perturbed level(s) should be much shorter than nearby rotational levels (or perhaps exhibit nonexponential decays). Although this possibility did not appear to be likely because the lifetime of nonperturbed levels pumped via the  $Q_1+Q_{p21}$  bandhead laser excitation did not exhibit any carrier gas pressure dependence, we deemed it prudent to measure the lifetimes as a function of rotational level pumped by the laser. Such a study may reveal variations not only at or near perturbed levels, but also interesting monotonic variations due to electronic transition moment dependence on internuclear distance. As will be seen, there is no large variation found near perturbed levels, indicating that collisional transfer out of the  $A^2\Sigma^+$  state through these levels is negligible. Thus, it would appear that nearly all of the excited state decay is due to radiative processes. The lifetimes reported herein are therefore directly indicative of the total radiative decay rate.

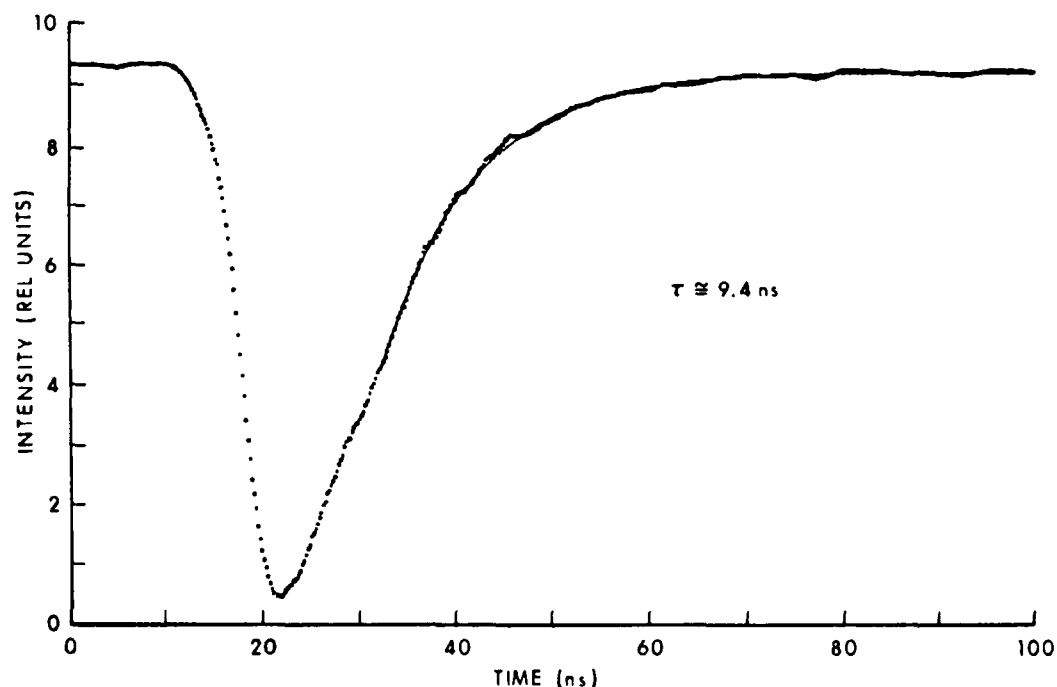


Figure 4. Fluorescence Decay Pulse from  $v'=0$  of the  $A^2\Sigma^+$  State.

As previously stated, the first lifetime measurements were made with the laser exciting PO in the  $Q_1+Q_{p21}$  bandhead. In order to obtain an estimate of the error limits in lifetimes, about 15 separate measurements of the A state lifetime were made upon pumping in this head. The resulting average lifetime

was  $9.72 \pm 0.48$  ns.\* Pumping in this head results in excitation of rotational levels near  $N'=5$ .<sup>6,7a</sup> Pumping in the  $P_1$  head leads to excitation<sup>6,7a</sup> of levels near  $N'=22$ . A similar number of runs was made for this bandhead, resulting in a lifetime of  $9.69 \pm 0.36$  ns. In addition, lifetimes were measured, using single runs, for all of the  $P_1$  branch transitions from  $P_{13}$  to  $P_{10}$ . (The rest of this vibrational band is too congested to allow for pumping of other single rotational levels at our resolution. See Figure 2.) This resulted in excitation of all  $N'$  levels between 2 and 9. It should be noted that the  $P_{10}$  transition is heavily overlapped by one component of the  $P_{11}$  line due to the perturbation of  $N'=10$ . Thus, there is a significant excitation of the perturbed  $N'=10$  level, as well as  $N'=9$ , upon pumping of the  $P_{10}$  line. No difference from the previously mentioned values was observed for any of these levels, including the perturbed level, within error limits. Now, in previous measurements on the  $B^2\Sigma^+$  state of PO, we have shown that although at 2 torr of Ar carrier gas some rotational relaxation may occur in the excited state, this relaxation should be far from complete. Thus, most of the emission must be either from the rotational level pumped by the laser or from nearby levels. This statement is also true for the  $A^2\Sigma^+$  state, especially since its lifetime is much shorter than that of the  $B^2\Sigma^+$  state (vide infra). There is thus less time for rotational relaxation to occur in the A state than in the B state under our conditions. Therefore, we conclude that the lifetimes do not depend upon rotational level within the limits of our measurement. The average of all the runs performed,  $9.68 \pm 0.47$  ns, is reported as the free radiative lifetime of the  $A^2\Sigma^+$  state. This result is in excellent agreement with the two previously reported measurements,  $11.5 \pm 2.0$  ns<sup>10</sup> and  $9 \pm 2$  ns.<sup>11a,b</sup> However, the agreement may be somewhat fortuitous because waveform digitizer distortion was not taken into account in the previous work. Also, note that the error limits from the previous work are much larger than those of the present work. The lifetime of the A state may be compared to measurements for the B state,  $250 \pm 10$  ns<sup>17</sup> and  $264.8 \pm 4.8$  ns.<sup>4</sup> One notes that the A state lifetime is much shorter than that of the B state even though radiative processes appear to be the major decay routes for each. The reason for the comparatively short A state lifetime will be discussed in the conclusions section.

Lifetimes were also studied as a function of carrier gas pressure. Whereas Ar was used as carrier gas for all of the other measurements, for this experiment Ar, and then He, was used as carrier gas. As previously mentioned, it was found that the lifetimes did not vary within error limits for either carrier gas. A pressure range from 0.5-10 torr was tried for both gases. These data may be used to place upper limits on the quenching rate constants,  $k_Q$ , of the  $A^2\Sigma^+$  state by these gases. The results are:  $k_{Q,Ar} \leq 3.1 \times 10^{-11}$  cm<sup>3</sup>/molecule-sec and  $k_{Q,He} \leq 3 \times 10^{-11}$  cm<sup>3</sup>/molecule-sec.

### C. $A^2\Sigma^+ \rightarrow X^2\Pi$ Electronic Transition Moment Function

In this section relative intensities of emission from  $v'=0$  of the  $A^2\Sigma^+$  state to the various  $v''$  levels in the  $X^2\Pi$  state are discussed. About 20 monochromator scans of the A-X system fluorescence, similar to that in

---

\*All error limits reported herein are one standard deviation.



Figure 3, were taken. Outputs from the monochromator's PMT and from the apparatus' monitor PMT were ratioed in the boxcar averager to correct for apparatus drift. The scans were taken using several different PMT voltages and two PO concentrations differing by a factor of 5 to determine whether detection system saturation or self absorption of the signal affected the results. Areas under the A-X system vibrational bands were integrated by the computer (trapezoidal summation). The results were then corrected for the detection system wavelength sensitivity. Finally, it should be noted that a monochromator scan was made with the discharge turned off (PO source off) in order to check for laser scattering in the vicinity of the (0,0) band. Signal from scattered laser radiation was negligible. Ratios of the band intensities were found to be identical within error limits under all conditions. Thus, detector system saturation and self-absorption effects are negligible. The results of all the scans were then averaged and ratioed to find the relative intensities of emission from  $v'=0$  in the A-X system. The relative intensities are directly proportional to the Einstein vibrational band emission coefficients,  $A_{v',v''}$ . The results may therefore be stated in terms of the relative emission coefficients, which are given in Table 1.

Table 1. Relative Einstein Band Emission Coefficients for  $v'=0$  in the  $A^2\Sigma^+-X^2\Pi$  System of PO

$(v',v'')$	$A_{v',v''}$ (Rel.)
(0,0)	1.000
(0,1)	$0.685 \pm 0.050$
(0,2)	$0.214 \pm 0.023$
(0,3)	$0.0443 \pm 0.0070$

The data in Table 1 may be used to investigate the dependence of the A-X electronic transition moment on internuclear distance. The same approach as used previously<sup>4</sup> to analyze data for the B-X transition was used here. Briefly, it is well known that the  $A_{v',v''}$  are given by

$$A_{v',v''} = (64\pi^4/2hc^3)\nu_{v',v''}^3 p_{v',v''} \quad (2)$$

where  $h$  is Planck's constant,  $c$  is the speed of light,  $\nu_{v',v''}$  is the band frequency and  $p_{v',v''}$  is the vibrational band transition probability. We assume that the electronic transition moment function,  $R_e(r)$ , is a linear function of internuclear distance,  $r$ , over the range of  $r$  of importance to the bands being considered. Thus,

$$R_e(r) = c(1 - \rho r) \quad (3)$$

where  $c$  and  $\rho$  are constants. Using this assumption, one can show<sup>4</sup> that

$$p_{v',v''} = c^2(1 - \rho \bar{r})^2 q_{v',v''} = R_e^2(\bar{r}) q_{v',v''} \quad (4)$$

where  $q_{v',v''}$  is the Franck-Condon factor (FCF) and  $\bar{r}$  the  $r$ -centroid for the vibrational band of interest. FCFs and  $r$ -centroids for the bands of interest were calculated using RKR potentials.  $p_{v',v''}$  values, normalized so that their total is equal to 1, may be readily calculated from the  $A_{v',v''}$  using Eq. 2.

Results for the  $p_{v',v''}$ , FCFs and r-centroids are given in Table 2. It is readily apparent from Eq. 4 that a plot of  $(p_{v',v''}/q_{v',v''})^{1/2}$  vs.  $\bar{r}$  will yield  $\rho$ . Such a plot is given in Figure 5. The result of a least squares fit, weighted by the error limits in the data points,<sup>18</sup> yields  $\rho = 0.627 \pm 0.039 \text{ \AA}^{-1}$ . This result is within error limits of that found using the FCFs and r-centroids of Sankaranarayanan.<sup>21</sup> The latter FCFs and r-centroids were calculated using Morse potentials and are similar to the RKR results for low  $v''$ , but differ progressively for high  $v''$ . Curiously, the value of  $\rho$  found for the A-X transition is very similar to that measured for the B-X system,<sup>4</sup>  $\rho = 0.577 \pm 0.010 \text{ \AA}^{-1}$ . We know of no reason why this has to be the case. An ab initio calculation would probably be required to elucidate whether this similarity arises merely from coincidence.

Table 2. Measured Vibrational Band Transition Probabilities and Calculated FCFs and r-centroids for the  $v'=0$  Progression in the A-X System of PO

Vibrational Band	Normalized $p_{v',v''}$ (Measured)	$q_{v',v''}$ (RKR Calc.)	$\bar{r}$ (Å) (RKR Calc.)
(0,0)	$0.484 \pm 0.013$	0.660	1.456
(0,1)	$0.364 \pm 0.025$	0.264	1.405
(0,2)	$0.125 \pm 0.014$	0.0626	1.357
(0,3)	$0.0282 \pm 0.0045$	0.0116	1.312

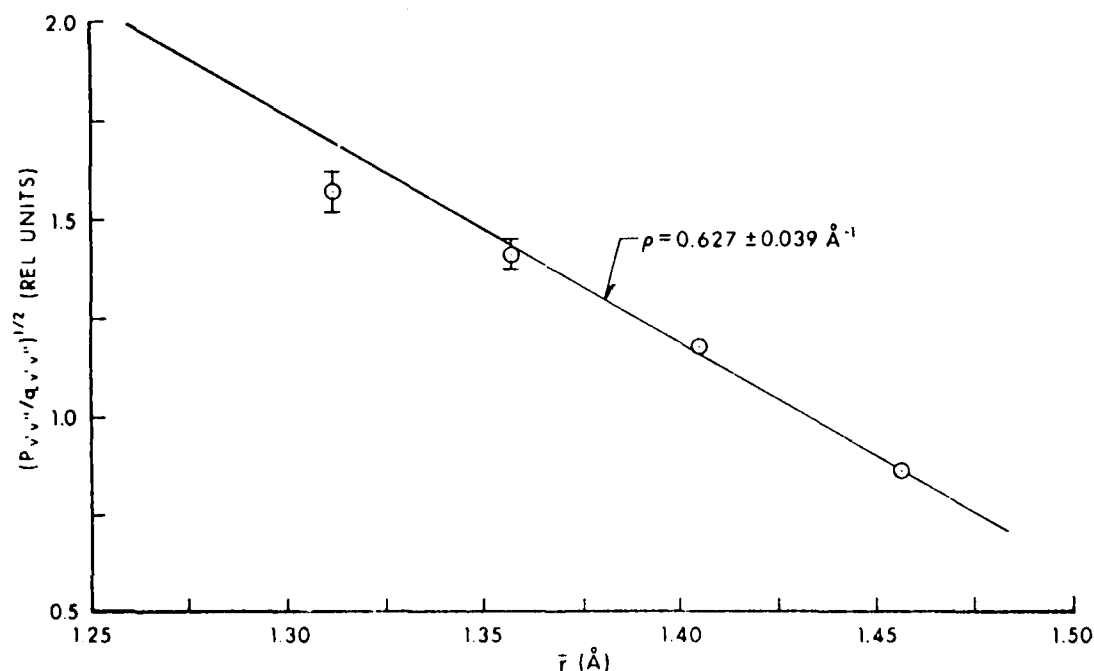


Figure 5. Plot of  $(p_{v',v''}/q_{v',v''})^{1/2}$  vs.  $\bar{r}$  for the  $v'=0$  Progression in the A-X System of PO. The line resulted from a least squares fit which was weighted for the error limits shown.

As one proceeds from low to high values of  $J'$ , centrifugal stretching will cause the value of  $p_{v',v''}$  to change slightly (see Eq. 4). Thus, for the value of  $\rho$  observed, the rate of radiative decay processes should decrease and lifetimes should increase as  $N'$  increases. The magnitude of this effect was investigated for the A-X transition in the same manner as was done previously for the B-X transition.<sup>4</sup> It should be noted here that when the A state is excited, most of the emission is to the X state rather than the B state (vide infra). Therefore, for the present purposes, the A-B emission may be neglected. The amount of centrifugal stretching for various values of  $J'$  was estimated using equations given by Herzberg.<sup>22</sup> Using Eq. 4, it is readily found that centrifugal stretching should cause a change in the lifetimes with  $J'$  that is much smaller than the error limits in these quantities. This is not surprising since the change for the B-X system was also too small to be detected. Relative error limits in the A state lifetime measurements are much larger than for the B state and the range of  $J'$  sampled for the A state is smaller than for the B state.

#### D. Relative Intensities of Emission from the $A^2\Sigma^+$ State to the $B^2\Sigma^+$ and $X^2\Pi$ States

After excitation of the A state of PO by the laser, the only allowed transitions in emission are to the B and X states (see Figure 1). The B state is indeed populated when the A state is excited, as shown by observation of B-X emission in Figure 3. For quantitative determination of PO via the A-X transition, it is necessary to know absolute values of the pertinent Einstein absorption and emission coefficients for this system. Before one can use the measured A state lifetime to calculate these quantities, one must obviously know the branching ratio for emission from the A state to the B and X states. Unfortunately, direct measurement of the A-B vs. A-X intensity ratio is very difficult because the (0,0) band of the A-B system occurs at about 10,300Å.<sup>12</sup> Most PMTs have very poor response at such long wavelengths.\* However, we have succeeded in measuring this ratio indirectly via the B-X vs A-X emission ratio.

As discussed previously, the B state may be populated after excitation of the A state by radiative or collisional processes. Since the B state emission is weak, there was some concern that a small fraction of the A state decay could be due to collisional processes and result in B state emission. However, clearly at zero pressure only radiative processes should occur. Therefore, in order to measure the A-B vs. A-X branching ratio indirectly, we measured the B-X vs. A-X intensity ratio as a function of pressure with the intent of extrapolating to zero pressure. (Along these lines, it is important to keep in mind that previous results<sup>4</sup> show that quenching, i.e., collisional transfer, of the B state by the Ar carrier gas is negligible in the pressure range used.) Note that the lifetimes of the A and B states are very different. The response time of the boxcar averager's preamplifier was much

---

\*In retrospect, it would appear from our results that attempts to detect the A-B emission directly with a PMT having an S1 photocathode might well succeed. We did not have such a PMT available for use at the time of these experiments.

too slow ( $\sim 1 \mu\text{s}$ ) to adequately follow pulsed signals from these states. Since distortion of signals from the two excited states probably would affect the signals in different ways, there was concern that the boxcar averager might not respond equally to the B-X and A-X fluorescence. (In fact, later comparison with the correct result indicates a very significant systematic error by about a factor of 5 is introduced). Therefore, the waveform digitizer, which is capable of following the two pulses without significant distortion, was used for these measurements. Excitation to the A state was again in the  $Q_1 + Q_{P21}$  head of the (0,0) band. The monochromator was centered alternately on the A-X and B-X (0,0) bands and was held fixed while signal from one of the transitions was averaged. At the same time, signal from the A-X monitor PMT, set up opposite the monochromator, was processed by the boxcar averager. The monochromator slits were set for a measured, trapezoidal bandpass of 41Å FWHM. Typically about 100 pulses were averaged. The A-X and B-X waveforms obtained from the digitizer were integrated from the beginning of the pulse to a sufficiently long time that the pulse had decayed to within error limits of zero intensity. The resulting integrals are proportional to the total number of photons emitted in the respective (0,0) bands of these systems. The integrals were corrected for system drift using the output from the A-X monitor PMT. It was found that the ratio of B-X and A-X signals did not vary at all, within error limits, between 1.3 and 8.0 torr of Ar carrier gas. This lack of pressure sensitivity means that all of the B-X emission results from A-B radiative transfer under our conditions, that is, collisional transfer is unimportant. Thus, the A-B vs. A-X emission ratio may be determined indirectly (but, we believe, quite accurately) from the ratio of integrated B-X vs. A-X signals.

The ratio of B-X vs. A-X signals was averaged for the 13 runs made at various Ar carrier gas pressures. The result was corrected for the measured detector system wavelength sensitivity. Also, the monochromator's bandpass function was measured and convoluted with the observed fluorescence spectrum from the (0,0) bands of the two electronic systems, (Figure 3) taken at much higher resolution, to obtain a further correction to the observed intensity ratio. Fortunately, the latter correction is not large and therefore is not particularly sensitive to the choice of several key parameters describing the high resolution fluorescence spectrum, i.e., the width of the two major peaks in each band and their separation. The resulting ratio of integrated signals for the B-X:A-X (0,0) bands was thus found to be  $0.216 \pm 0.026:1.000$ . It may be shown using FCFs calculated from the RKR curves that for the A-B transition, most of the emission from  $v=0$  in the A state is to  $v=0$  in the B state. Some emission to  $v=1$  occurs. The (1,1) and (1,2) bands are at about the same wavelengths as the (0,0) and (0,1) bands, respectively. Using results for the B-X electronic transition moment function from Ref. 4, one may readily show that the ratio of B-X (1,1):(1,2) intensities is similar to that of (0,0):(0,1). The (1,0) intensity and intensities for other (1, $v''$ ) bands are expected to be negligible in comparison. Therefore, even though  $v=1$  of the B state is slightly populated, the system response to emission from this level is expected to be approximately equivalent to that from  $v=0$ . Emission to (and from) higher vibrational levels of the B state is expected to have a negligible effect on the result. Thus, the ratio of total Einstein emission coefficients for the A-B vs. A-X transitions may be obtained from the B-X:A-X (0,0) band ratio using the relative intensities of the  $v'=0$  progressions in the A-X and B-X systems. The former intensities are given in the preceding section while the latter may be obtained from previous work.<sup>3</sup> The ratio of

total Einstein emission coefficients thus obtained for the two electronic systems is  $A_{AB}/A_{AX} = 0.120 \pm 0.016$ . It is interesting to note that although the intensity of the A-X transition is actually stronger than that of the A-B transition, after the  $\nu^3$  dependence is removed from the intensity ratio one finds that the square of the electronic transition moment for the A-B transition is almost 10 times that of the A-X transition.

#### IV. CONCLUSIONS

LIF of the PO radical is readily produced by excitation of the radical in the A-X system after its formation in a microwave discharge. Fluorescence and excitation scans from which the A-X transition may be readily identified are given in this work. The A state was found to have a very short excited state lifetime. Its lifetime is, for instance, much shorter than the B state lifetime. The lifetime was found to be independent of rotational level excited. Relative intensities of emission from  $\nu=0$  of the A state to the various vibrational levels in the ground state were used to examine the variation of the A-X electronic transition moment with internuclear distance. The branching ratio for emission from the A state to the B and X states was determined by an indirect method. The branching ratio and A state lifetime, taken together with the fact that the A state decays primarily via radiative processes, indicate that both the A-X and A-B transitions are very strong. The strength of these transitions may at first glance be somewhat surprising. However, studies of Verma and coworkers<sup>8,23</sup> show that the  $A^2\Sigma^+$  state fits very well into the Rydberg series leading to  $PO^+ ({}^1\Sigma^+)$ . This state corresponds to having one electron in the  $4s\sigma$  orbital, i.e., it is the lowest state in the  $ns\sigma$  series. The  $B^2\Sigma^+$  state does not fit into these Rydberg series. Thus, experimental evidence would seem to indicate that it is a valence state. Recent ab initio calculations of Grein and Kapur<sup>24</sup> support this classification. Therefore, both the A-X and A-B transitions may be classified as Rydberg transitions. As discussed by Herzberg,<sup>25</sup> Rydberg transitions of molecules are expected to be very strong, in analogy with atomic Rydberg transitions. The strength of these transitions is therefore reasonable. Given equal probe intensities at the respective transition wavelengths and linear responses, one would expect detection schemes to be much more sensitive if based upon pumping the A-X transition than if based on the B-X transition. This observation agrees with the results of Ref. 9.

The ability to pump the A state and view fluorescence from both this state and the B state suggests the possibility of performing interesting electronic energy transfer experiments with the PO molecule. At the present, although there have been many studies of electronic quenching, few experimental studies on electronic energy transfer between the excited states of molecules have been performed. Though some other low-lying electronic levels might also be of importance in such experiments, (see Figure 1) this molecule nevertheless could lend itself to such a study. Such studies could be especially interesting because of transfer between different Rydberg levels.

#### ACKNOWLEDGEMENTS

Financial support and the loan of the Raman shifter by the Chemical Research, Development and Engineering Center are gratefully acknowledged.

## REFERENCES

1. See papers in Proceedings of the 1983 Scientific Conference on Chemical Defense Research, R.L. Dimmick, Jr. and M. Rausa, eds., CRDC Special Publication CRDC-SP-84014, October 1984.
2. R.J. VanZee and A.U. Khan, "Transient Emitting Species in Phosphorus Chemiluminescence," J. Chem. Phys., Vol. 65, p. 1764, 1976.
3. W.R. Anderson, S.W. Bunte, and A.J. Kotlar, "Measurement of Franck-Condon Factors for the  $v'=0$  Progression in the B-X System of PO," Chem. Phys. Lett., Vol. 110, p. 145, 1984.
4. K.N. Wong, W.R. Anderson, A.J. Kotlar, M.A. DeWilde, and L.J. Decker, "Lifetimes and Quenching of  $B^2\Sigma^+ PO$  by Atmospheric Gases," J. Chem. Phys., Vol. 84, p. 81, 1986.
5. S.R. Long, A.W. Miziolek, and M.A. DeWilde, "Laser Induced Fragmentation of CW Agents," Proceedings of the 1983 Scientific Conference on Chemical Defense Research, R.L. Dimmick, Jr. and M. Rausa, eds., Special Report CRDC-SP-84014, October 1984.
6. K. Suryanarayana Rao, "Rotational Analysis of the  $\gamma$  System of the PO Molecule," Can. J. Phys., Vol. 36, p. 1526, 1958.
- 7a. B. Coquart, C. Couet, T.A. Ngo, and H. Guenebaut, "Contribution A L'etude des Systemes Electroniques du Radical PO. 2<sup>e</sup> Partie: Considerations Nouvelles Sur le Systeme  $\gamma$  (Transition  $A^2\Sigma^+-X^2\Pi$ )," J. Chim. Phys., Vol. 64, p. 1197, 1967.
- b. B. Coquart and J.C. Prudhomme, "Reconsiderations Sue le Systeme  $\gamma$  de PO; Localization de Perturbations Rotationelles. Dans Les Premiers Niveaux Vibrationnels de L'etat  $A^2\Sigma^+$ ," C.R. Acad. Sci., Vol. B275, p. 383, 1972.
- c. B. Coquart, M. DaPaz, and J.C. Prudhomme, "Transition  $A^2\Sigma^+-X^2\Pi$  des Molecules  $P^{16}O$  et  $P^{18}O$ . Pertubations de L'etat  $A^2\Sigma^+$ ," Can. J. Phys., Vol. 53, 377, 1975.
8. S.N. Ghosh and R.D. Verma, "Rydberg States of the PO Molecule," J. Mol. Spectrosc., Vol. 72, 200, 1978.
- 9a. H. Haraguchi, W.K. Fowler, D.J. Johnson, and J.D. Winefordner, "Molecular Fluorescence Spectroscopy of Phosphorus Monoxide in Flames Studied by a SIT-OMA System," Spectrochim. Acta, Vol. 32A, p. 1539, 1976.
- b. D.J. Johnson, W.K. Fowler, and J.D. Winefordner, "Evaluation of a Pulsed EIMAC Source for Atomic Fluorescence Spectrometry," Talanta, Vol. 24, p. 227, 1977.
- c. W.K. Fowler and J.D. Winefordner, "Background Fluorescence Spectra Observed in Atomic Fluorescence Spectrometry with a Continuum Source," Anal. Chem., Vol. 49, p. 944, 1977.

- 10a. W.R. Anderson, L.J. Decker, and A.J. Kotlar, "Measurement of a Spectral Data Base for the PO Radical," Proceedings of the 1983 Scientific Conference on Chemical Defense Research, Special Report CRDC-SP-84014, October 1984.
- b. W.R. Anderson, L.J. Decker, A.J. Kotlar, and M.A. DeWilde, "Laser Excited Fluorescence Studies of the PO Radical," 39th Symposium on Molecular Spectroscopy, Columbus, OH, Paper RC8, June 1984.
- 11a. S.R. Long, R.C. Sausa, and A.W. Miziolek, "Laser-Induced Fluorescence Studies of PO Generated by UV Laser Photofragmentation of DMMP," Proceedings of 1984 Scientific Conference on Chemical Defense Research, Special Publication CRDC-SP-85006, June 1985.
- b. S.R. Long, R.C. Sausa, and A.W. Miziolek, "LIF Studies of PO Produced in Excimer Laser Photolysis of Dimethylmethylphosphonate," Chem. Phys. Lett., Vol. 117, p. 505, 1985.
- c. R.C. Sausa, A.W. Miziolek, and S.R. Long, "State Distributions, Quenching, and Reaction of PO Radical Generated in Excimer Laser Photofragmentation of Dimethyl Methylphosphonate," to appear in J. Phys. Chem.
12. R.D. Verma and S.S. Jois, "Emission Spectrum of the PO Molecule. Part IV. Spectrum in the Region 7,000-12,000Å," Can. J. Phys., Vol. 51, p. 322, 1973.
13. P.N. Ghosh and G.N. Ball, "Die Ultravioletten Banden des Phosphoroxys," Z. Physik, Vol. 71, p. 362, 1931.
14. N.L. Singh, "Rotational Analysis of the  $\beta$  Bands of Phosphorus Monoxide," Can. J. Phys., Vol. 37, p. 136, 1959.
15. R.D. Verma and S.R. Singhal, "New Results on the  $B^2\Sigma^+$ ,  $b^4\Sigma^-$ , and  $X^2\Pi$  States of PO," Can. J. Phys., Vol. 53, p. 411, 1975.
16. C. Couet, N. Tuan Anh, B. Coquart, and H. Guenebaut, "Contribution a L'Etude des Systemes Electroniques du Radical PO: 3e Partie: Le Systeme  $\beta$  (Transition  $B^2\Sigma^+-X^2\Pi_r$ )," J. Chim. Phys., Vol. 65, p. 217, 1968.
17. M.A.A. Clyne and M.C. Heaven, "Laser-Induced Fluorescence of the PO Radical," Chem. Phys., Vol. 58, p. 145, 1981.
18. W.E. Wentworth, "Rigorous Least Squares Adjustment; Application to Some Nonlinear Equations, I," J. Chem. Ed., Vol. 42, p. 96, 1965.
19. J.N. Demas, Excited State Lifetime Measurements, Chapter 7, Section C, Academic Press, New York, 1983.
20. T. Iwai, M.I. Savadatti, and H.P. Broida, "Mechanisms of Populating Electronically Excited CN in Active Nitrogen Flames," J. Chem. Phys., Vol. 47, p. 3861, 1967, and references therein.



21. S. Sankaranarayanan, "r-centroids and Franck-Condon Factors for the Bands of the  $A^2\Sigma-X^2\Pi$  System of PO Molecule," Indian J. Phys., Vol. 40, p. 678, 1967.
22. G. Herzberg, Molecular Spectra and Molecular Structure. I. Spectra of Diatomic Molecules, Van Nostrand Reinhold, New York, p. 104, 1950.
23. R.D. Verma, M.N. Dixit, S.S. Jois, S. Nagaraj, and S.R. Singhal, "Emission Spectrum of the PO Molecule. Part II.  $^2\Sigma-^2\Sigma$  Transitions," Can. J. Phys., Vol. 49, p. 3180, 1971.
24. F. Grein and A. Kapur, "Configuration Interaction Studies on Low-Lying Valence and Rydberg States of PO," J. Chem. Phys., Vol. 78, p. 339, 1983.
25. G. Herzberg, Molecular Spectra and Molecular Structure. I. Spectra of Diatomic Molecules, Van Nostrand Reinhold, New York, p. 383, 1950.

# DISTRIBUTION LIST

<u>No. Of Copies</u>	<u>Organization</u>	<u>No. Of Copies</u>	<u>Organization</u>
12	Administrator Defense Technical Info Center ATTN: DTIC-DDA Cameron Station Alexandria, VA 22304-6145	1	Commander US Army Aviation Research and Development Command ATTN: AMSAV-E 4300 Goodfellow Blvd. St. Louis, MO 63120
1	HQ DA DAMA-ART-M Washington, DC 20310	1	Director US Army Air Mobility Research and Development Laboratory Ames Research Center Moffett Field, CA 94035
1	Commander US Army Materiel Command ATTN: AMCDRA-ST 5001 Eisenhower Avenue Alexandria, VA 22333-0001	4	Commander US Army Research Office ATTN: R. Ghirardelli D. Mann R. Singleton R. Shaw P.O. Box 12211 Research Triangle Park, NC 27709-2211
10	Central Intelligence Agency Office of Central Reference Dissemination Branch Room GE-47 HQS Washington, DC 20502		
1	Commander Armament R&D Center US Army AMCCOM ATTN: SMCAR-TSS Dover, NJ 07801	1	Commander US Army Communications - Electronics Command ATTN: AMSEL-ED Fort Monmouth, NJ 07703
1	Commander Armament R&D Center US Army AMCCOM ATTN: SMCAR-TDC Dover, NJ 07801	1	Commander ERADCOM Technical Library ATTN: DELSD-L, Reports Section Fort Monmouth, NJ 07703-5301
1	Director Benet Weapons Laboratory Armament R&D Center US Army AMCCOM ATTN: SMCAR-LCB-TL Watervliet, NY 12189	2	Commander Armament R&D Center US Army AMCCOM ATTN: SMCAR-LCA-G, D.S. Downs J.A. Lannon Dover, NJ 07801
1	Commander US Army Armament, Munitions and Chemical Command ATTN: SMCAR-ESP-L Rock Island, IL 61299	1	Commander Armament R&D Center US Army AMCCOM ATTN: SMCAR-LC-G, L. Harris Dover, NJ 07801

# DISTRIBUTION LIST

<u>No. Of Copies</u>	<u>Organization</u>	<u>No. Of Copies</u>	<u>Organization</u>
1	Commander Armament R&D Center US Army AMCCOM ATTN: SMCAR-SCA-T, L. Stiefel Dover, NJ 07801	1	Commander US Army Development and Employment Agency ATTN: MODE-TED-SAB Fort Lewis, WA 98433
1	Commander US Army Missile Command Research, Development and Engineering Center ATTN: AMSMI-RD Redstone Arsenal, AL 35898	1	Office of Naval Research Department of the Navy ATTN: R.S. Miller, Code 432 800 N. Quincy Street Arlington, VA 22217
1	Commander US Army Missile and Space Intelligence Center ATTN: AIAMS-YDL Redstone Arsenal, AL 35898-5000	1	Commander Naval Air Systems Command ATTN: J. Ramnarace, AIR-54111C Washington, DC 20360
2	Commander US Army Missile Command ATTN: AMSMI-RK, D.J. Ifshin W. Wharton Redstone Arsenal, AL 35898	2	Commander Naval Ordnance Station ATTN: C. Irish P.L. Stang, Code 515 Indian Head, MD 20640
1	Commander US Army Missile Command ATTN: AMSMI-RKA, A.R. Maykut Redstone Arsenal, AL 35898-5249	1	Commander Naval Surface Weapons Center ATTN: J.L. East, Jr., G-23 Dahlgren, VA 22448-5000
1	Commander US Army Tank Automotive Command ATTN: AMSTA-TSL Warren, MI 48397-5000	2	Commander Naval Surface Weapons Center ATTN: R. Bernecker, R-13 G.B. Wilmot, R-16 Silver Spring, MD 20902-5000
1	Director US Army TRADOC Systems Analysis Activity ATTN: ATAA-SL White Sands Missile Range, NM 88002	1	Commander Naval Weapons Center ATTN: R.L. Derr, Code 389 China Lake, CA 93555
1	Commandant US Army Infantry School ATTN: ATSH-CD-CSO-OR Fort Benning, GA 31905	2	Commander Naval Weapons Center ATTN: Code 3891, T. Boggs K.J. Graham China Lake, CA 93555

# DISTRIBUTION LIST

<u>No. Of Copies</u>	<u>Organization</u>	<u>No. Of Copies</u>	<u>Organization</u>
5	Commander Naval Research Laboratory ATTN: M.C. Lin J. McDonald E. Oran J. Shnar R.J. Doyle, Code 6110 Washington, DC 20375	1	NASA Langley Research Center Langley Station ATTN: G.B. Northam/MS 168 Hampton, VA 23365
1	Commanding Officer Naval Underwater Systems Center Weapons Dept. ATTN: R.S. Lazar/Code 36301 Newport, RI 02840	4	National Bureau of Standards ATTN: J. Hastie M. Jacox T. Kashiwagi H. Semerjian US Department of Commerce Washington, DC 20234
1	Superintendent Naval Postgraduate School Dept. of Aeronautics ATTN: D.W. Netzer Monterey, CA 93940	1	OSD/SDIO/UST ATTN: L.H. Caveny Pentagon Washington, DC 20301-7100
4	AFRPL/DY, Stop 24 ATTN: R. Corley R. Geisler J. Levine D. Weaver Edwards AFB, CA 93523-5000	1	Aerojet Solid Propulsion Co. ATTN: P. Micheli Sacramento, CA 95813
1	AFRPL/MKPB, Stop 24 ATTN: B. Goshgarian Edwards AFB, CA 93523-5000	1	Applied Combustion Technology, Inc. ATTN: A.M. Varney P.O. Box 17885 Orlando, FL 32860
1	AFOSR ATTN: J.M. Tishkoff Bolling Air Force Base Washington, DC 20332	2	Applied Mechanics Reviews The American Society of Mechanical Engineers ATTN: R.E. White A.B. Wenzel 345 E. 47th Street New York, NY 10017
1	Air Force Armament Laboratory ATTN: AFATL/DLODL Eglin AFB, FL 32542-5000	1	Atlantic Research Corp. ATTN: M.K. King 5390 Cherokee Avenue Alexandria, VA 22314
1	Air Force Weapons Laboratory AFWL/4JL ATTN: V. King Kirtland AFB, NM 87117	1	Atlantic Research Corp. ATTN: R.H.W. Waesche 7511 Wellington Road Gainesville, VA 22065

# DISTRIBUTION LIST

<u>No. Of Copies</u>	<u>Organization</u>	<u>No. Of Copies</u>	<u>Organization</u>
1	AVCO Everett Rsch. Lab. Div. ATTN: D. Stickler 2385 Revere Beach Parkway Everett, MA 02149	1	General Electric Ordnance Systems ATTN: J. Mandzy 100 Plastics Avenue Pittsfield, MA 01203
1	Battelle Memorial Institute Tactical Technology Center ATTN: J. Huggins 505 King Avenue Columbus, OH 43201	2	General Motors Rsch Labs Physics Department ATTN: T. Sloan R. Teets Warren, MI 48090
1	Cohen Professional Services ATTN: N.S. Cohen 141 Channing Street Redlands, CA 92373	2	Hercules, Inc. Allegany Ballistics Lab. ATTN: R.R. Miller E.A. Yount P.O. Box 210 Cumberland, MD 21501
1	Exxon Research & Eng. Co. Government Research Lab ATTN: A. Dean P.O. Box 48 Linden, NJ 07036	1	Hercules, Inc. Bacchus Works ATTN: K.P. McCarty P.O. Box 98 Magna, UT 84044
1	Ford Aerospace and Communications Corp. DIVAD Division Div. Hq., Irvine ATTN: D. Williams Main Street & Ford Road Newport Beach, CA 92663	1	Honeywell, Inc. Government and Aerospace Products ATTN: D.E. Broden/ MS MN50-2000 600 2nd Street NE Hopkins, MN 55343
1	General Applied Science Laboratories, Inc. ATTN: J.I. Erdos 425 Merrick Avenue Westbury, NY 11590	1	IBM Corporation ATTN: A.C. Tam Research Division 5600 Cottle Road San Jose, CA 95193
1	General Electric Armament & Electrical Systems ATTN: M.J. Bulman Lakeside Avenue Burlington, VT 05401	1	IIT Research Institute ATTN: R.F. Remaly 10 West 35th Street Chicago, IL 60616
1	General Electric Company 2352 Jade Lane Schenectady, NY 12309		

# DISTRIBUTION LIST

<u>No. Of Copies</u>	<u>Organization</u>	<u>No. Of Copies</u>	<u>Organization</u>
2	Director Lawrence Livermore National Laboratory ATTN: C. Westbrook M. Costantino P.O. Box 808 Livermore, CA 94550	1	Rockwell International Corp. Rocketdyne Division ATTN: J.E. Flanagan/HB02 6633 Canoga Avenue Canoga Park, CA 91304
1	Lockheed Missiles & Space Co. ATTN: George Lo 3251 Hanover Street Dept. 52-35/B204/2 Palo Alto, CA 94304	4	Sandia National Laboratories Combustion Sciences Dept. ATTN: R. Cattolica S. Johnston P. Mattern D. Stephenson Livermore, CA 94550
1	Los Alamos National Lab ATTN: B. Nichols T7, MS-B284 P.O. Box 1663 Los Alamos, NM 87545	1	Science Applications, Inc. ATTN: R.B. Edelman 23146 Cumorah Crest Woodland Hills, CA 91364
1	National Science Foundation ATTN: A.B. Harvey Washington, DC 20550	1	Science Applications, Inc. ATTN: H.S. Pergament 1100 State Road, Bldg. N Princeton, NJ 08540
1	Olin Corporation Smokeless Powder Operations ATTN: V. McDonald P.O. Box 222 St. Marks, FL 32355	3	SRI International ATTN: G. Smith D. Crosley D. Golden 333 Ravenswood Avenue Menlo Park, CA 94025
1	Paul Gough Associates, Inc. ATTN: P.S. Gough 1048 South Street Portsmouth, NH 03801	1	Stevens Institute of Tech. Davidson Laboratory ATTN: R. McAlevy, III Hoboken, NJ 07030
2	Princeton Combustion Research Laboratories, Inc. ATTN: M. Summerfield N.A. Messina 475 US Highway One Monmouth Junction, NJ 08852	1	Textron, Inc. Bell Aerospace Co. Division ATTN: T.M. Ferger P.O. Box 1 Buffalo, NY 14240
1	Hughes Aircraft Company ATTN: T.E. Ward 8433 Fallbrook Avenue Canoga Park, CA 91303	1	Thiokol Corporation Elkton Division ATTN: W.N. Brundige P.O. Box 241 Elkton, MD 21921

# DISTRIBUTION LIST

<u>No. Of Copies</u>	<u>Organization</u>	<u>No. Of Copies</u>	<u>Organization</u>
1	Thiokol Corporation Huntsville Division ATTN: R. Glick Huntsville, AL 35807	1	Brigham Young University Dept. of Chemical Engineering ATTN: M.W. Beckstead Provo, UT 84601
3	Thiokol Corporation Wasatch Division ATTN: S.J. Bennett P.O. Box 524 Brigham City, UT 84302	1	California Institute of Tech. Jet Propulsion Laboratory ATTN: MS 125/159 4800 Oak Grove Drive Pasadena, CA 91103
1	TRW ATTN: M.S. Chou MSR1-1016 1 Parke Redondo Beach, CA 90278	1	California Institute of Technology ATTN: F.E.C. Culick/ MC 301-46 204 Karman Lab. Pasadena, CA 91125
1	United Technologies ATTN: A.C. Eckbreth East Hartford, CT 06108	1	University of California, Berkeley Mechanical Engineering Dept. ATTN: J. Daily Berkeley, CA 94720
3	United Technologies Corp. Chemical Systems Division ATTN: R.S. Brown T.D. Myers (2 copies) P.O. Box 50015 San Jose, CA 95150-0015	1	University of California Los Alamos Scientific Lab. P.O. Box 1663, Mail Stop B216 Los Alamos, NM 87545
2	United Technologies Corp. ATTN: R.S. Brown R.O. McLaren P.O. Box 358 Sunnyvale, CA 94086	2	University of California, Santa Barbara Quantum Institute ATTN: K. Schofield M. Steinberg Santa Barbara, CA 93106
1	Universal Propulsion Company ATTN: H.J. McSpadden Black Canyon Stage 1 Box 1140 Phoenix, AZ 85029	2	University of Southern California Dept. of Chemistry ATTN: S. Benson C. Wittig Los Angeles, CA 90007
1	Veritay Technology, Inc. ATTN: E.B. Fisher 4845 Millersport Highway P.O. Box 305 East Amherst, NY 14051-0305	1	Case Western Reserve Univ. Div. of Aerospace Sciences ATTN: J. Tien Cleveland, OH 44135

# DISTRIBUTION LIST

<u>No. Of Copies</u>	<u>Organization</u>	<u>No. Of Copies</u>	<u>Organization</u>
1	Cornell University Department of Chemistry ATTN: T.A. Cool Baker Laboratory Ithaca, NY 14853	3	Pennsylvania State University Applied Research Laboratory ATTN: K.K. Kuo H. Palmer M. Micci University Park, PA 16802
1	Univ. of Dayton Rsch Inst. ATTN: D. Campbell AFRPL/PAP Stop 24 Edwards AFB, CA 93523	1	Polytechnic Institute of NY Graduate Center ATTN: S. Lederman Route 110 Farmingdale, NY 11735
1	University of Florida Dept. of Chemistry ATTN: J. Winefordner Gainesville, FL 32611	2	Princeton University Forrestal Campus Library ATTN: K. Brezinsky I. Glassman P.O. Box 710 Princeton, NJ 08540
3	Georgia Institute of Technology School of Aerospace Engineering ATTN: E. Price W.C. Strahle B.T. Zinn Atlanta, GA 30332	1	Princeton University MAE Dept. ATTN: F.A. Williams Princeton, NJ 08544
1	University of Illinois Dept. of Mech. Eng. ATTN: H. Krier 144MEB, 1206 W. Green St. Urbana, IL 61801	1	Purdue University School of Aeronautics and Astronautics ATTN: J.R. Osborn Grissom Hall West Lafayette, IN 47906
1	Johns Hopkins University/APL Chemical Propulsion Information Agency ATTN: T.W. Christian Johns Hopkins Road Laurel, MD 20707	1	Purdue University Department of Chemistry ATTN: E. Grant West Lafayette, IN 47906
1	University of Michigan Gas Dynamics Lab Aerospace Engineering Bldg. ATTN: G.M. Faeth Ann Arbor, MI 48109-2140	2	Purdue University School of Mechanical Engineering ATTN: N.M. Laurendeau S.N.B. Murthy TSPC Chaffee Hall West Lafayette, IN 47906
1	University of Minnesota Dept. of Mechanical Engineering ATTN: E. Fletcher Minneapolis, MN 55455	1	Rensselaer Polytechnic Inst. Dept. of Chemical Engineering ATTN: A. Fontijn Troy, NY 12181



# DISTRIBUTION LIST

<u>No. Of Copies</u>	<u>Organization</u>
1	Stanford University Dept. of Mechanical Engineering ATTN: R. Hanson Stanford, CA 94305
1	University of Texas Dept. of Chemistry ATTN: W. Gardiner Austin, TX 78712
1	University of Utah Dept. of Chemical Engineering ATTN: G. Flandro Salt Lake City, UT 84112
1	Virginia Polytechnic Institute and State University ATTN: J.A. Schetz Blacksburg, VA 24061
1	Commandant USAFAS ATTN: ATSF-TSM-CN Fort Sill, OK 73503-5600

## Aberdeen Proving Ground

Dir, USAMSAA  
ATTN: AMXSY-D  
AMXSY-MP, H. Cohen  
Cdr, USATECOM  
ATTN: AMSTE-TO-F  
Cdr, CRDC, AMCCOM  
ATTN: SMCCR-RSP-A  
SMCCR-MU  
SMCCR-SPS-IL

# USER EVALUATION SHEET/CHANGE OF ADDRESS

This Laboratory undertakes a continuing effort to improve the quality of the reports it publishes. Your comments/answers to the items/questions below will aid us in our efforts.

1. BRL Report Number \_\_\_\_\_ Date of Report \_\_\_\_\_

2. Date Report Received \_\_\_\_\_

3. Does this report satisfy a need? (Comment on purpose, related project, or other area of interest for which the report will be used.) \_\_\_\_\_  
\_\_\_\_\_  
\_\_\_\_\_

4. How specifically, is the report being used? (Information source, design data, procedure, source of ideas, etc.) \_\_\_\_\_  
\_\_\_\_\_  
\_\_\_\_\_

5. Has the information in this report led to any quantitative savings as far as man-hours or dollars saved, operating costs avoided or efficiencies achieved, etc? If so, please elaborate. \_\_\_\_\_  
\_\_\_\_\_  
\_\_\_\_\_

6. General Comments. What do you think should be changed to improve future reports? (Indicate changes to organization, technical content, format, etc.) \_\_\_\_\_  
\_\_\_\_\_  
\_\_\_\_\_

CURRENT ADDRESS	_____
	Name
	_____
	Organization
	_____
	Address
	_____
	City, State, Zip

7. If indicating a Change of Address or Address Correction, please provide the New or Correct Address in Block 6 above and the Old or Incorrect address below.

OLD ADDRESS	_____
	Name
	_____
	Organization
	_____
	Address
	_____
	City, State, Zip

(Remove this sheet along the perforation, fold as indicated, staple or tape closed, and mail.)

----- FOLD HERE -----

Director  
U.S. Army Ballistic Research Laboratory  
ATTN: SLCBR-DD-T  
Aberdeen Proving Ground, MD 21005-5066

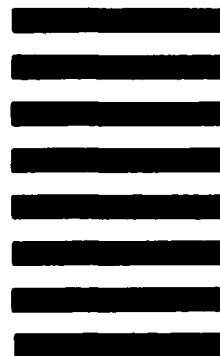


NO POSTAGE  
NECESSARY  
IF MAILED  
IN THE  
UNITED STATES

OFFICIAL BUSINESS  
PENALTY FOR PRIVATE USE, \$300

**BUSINESS REPLY MAIL**  
FIRST CLASS PERMIT NO 12062 WASHINGTON, DC  
POSTAGE WILL BE PAID BY DEPARTMENT OF THE ARMY

Director  
U.S. Army Ballistic Research Laboratory  
ATTN: SLCBR-DD-T  
Aberdeen Proving Ground, MD 21005-9989



----- FOLD HERE -----

END

1-87

DTIC